EPJ Photovoltaics **16**, 16 (2025)
© P. Hacke et al., Published by EDP Sciences, 2025
https://doi.org/10.1051/epjpv/2025004

Available online at:
www.epj-pv.org

Special Issue on 'EU PVSEC 2024: State of the Art and Developments in Photovoltaics', edited by Robert Kenny and Gabriele Eder

ORIGINAL ARTICLE OPEN ACCESS

Polarization-type potential-induced degradation in bifacial PERC modules in the field

Peter Hacke[1,*], Cecile Molto[2], Dylan Colvin[2], Ryan Smith[3], Farrukh Ibne Mahmood[4], Fang Li[4], Jaewon Oh[5], Govindasamy Tamizhmani[4], and Hubert Seigneur[2]

[1] National Renewable Energy Laboratory, Golden, CO 80401, USA
[2] Florida Solar Energy Center – University of Central Florida, Cocoa, FL 32922, USA
[3] Pordis LLC, Austin, TX 78729, USA
[4] Photovoltaic Reliability Laboratory – Arizona State University, Mesa, AZ 85212, USA
[5] University of North Carolina at Charlotte, Charlotte, NC 28223, USA

Received: 20 September 2024 / Accepted: 14 January 2025

Abstract. This study examines the susceptibility of bifacial glass/glass passivated emitter and rear cell (PERC) modules to potential-induced degradation-polarization (PID-p) in the field. While there are several studies showing PID-p occurring on both front and back faces of bifacial PERC in accelerated tests, we address the yet unclarified behavior in fielded modules. We examine the effects of mounting configuration; specifically, comparing modules mounted near ground and in elevated ground rack configurations. Modules with the cell circuit in −1500 V system voltage configuration, whether mounted on racks about 30 cm above the ground or elevated 2 m high showed mean degradation of 4.5% to 6% in power under standard test conditions over about 2.5 weeks as measured from the front side of the module. This extent of degradation remained sustained for a duration of about 6 months analyzed. Average daytime temperatures of modules in the various mounting configurations were similar and therefore judged to be insufficient to be a primary influence for the modest PID-p rate differences that we observed among mounting configurations. Increased leakage current in the morning suggests morning dew was sustained longer on modules near the ground measured over six months which would be expected to increase the PID-p rate over the long term. However, the main difference seen between the modules on the various mountings during the initial period with up to 6% mean degradation by PID-p was the approximately two times the irradiance from albedo on the rear of modules mounted in elevated ground rack compared to those on the near ground rack. This difference in incident albedo led to a modestly reduced rate of the development of PID-p of the modules on the elevated ground rack. The difference is attributed to the dissipation of PID-p-causing electrical charge by the albedo incident on the module rear. The behavior could be modeled by a sigmoidal equation with consideration of the differences in the insolation on the module rear.

Keywords: Photovoltaics / photovoltaic modules / reliability / potential-induced degradation

1 Introduction

PID-polarization (PID-p) involves motion of charge into or out of the dielectric passivation layers of solar cells such that more minority carriers drift from the semiconductor to its interface with the dielectric [1]. This leads to more minority carrier recombination at that interface resulting in reduced photocurrent and voltage [2,3]. The mechanisms of the polarization effect are not uniquely clarified. Charge species may be a static charge or k-centers in silicon nitride [4] that can be dissipated by UV irradiation because of the resulting photoconductivity in the dielectric [5,6], but there are cases where the effect seems to not be dissipated with UV irradiation [7] and we may speculate an ionic charge could be involved in some cases. PID-p can occur on the rear side in bifacial PERC modules based on tests in damp heat or with foil applied on the surfaces of the glass with the cells in negative potential [2,8]. There are publications indicating sensitivity in positive bias on the front side as well [8–10]. There is also a study showing PID-p occurring on the rear of bifacial PERC with the combined effects of negative system voltage bias, moisture, and illumination that are applied in realistic levels in combined-accelerated

* e-mail: peter.hacke@nrel.gov

This is an Open Access article distributed under the terms of the Creative Commons Attribution License (https://creativecommons.org/licenses/by/4.0), which permits unrestricted use, distribution, and reproduction in any medium, provided the original work is properly cited.

stress testing (CAST), which indicates that PID-p can occur in fielded PERC modules [11]. There are however no field studies we know of reporting PID-p in bifacial PERC modules occurring in the natural environment along with the rates and modeling of such rates based on the stress factors that the modules experience. This study therefore examines the susceptibility of bifacial glass/glass PERC modules with frames to PID-p in ground-mounted PV systems. We examine the effects of mounting configuration, comparing modules mounted near ground and in elevated ground rack conditions.

Modeling of the PID behavior of PID-shunting has been performed, including with the use of sigmoidal equations [12], exponential and power law analyses [13]. The PID-p rate has been modeled with a sigmoidal analysis considering the balance of charge driven to the dielectric along with dissipation by light for passivated emitter rear totally diffused (PERT) cell modules with p^+n fronts, which have a similar front structure to TOPCon-type cells [14,15]. Rates of PID-p were extensively studied in PERT cells by Yamaguchi and coworkers in accelerated testing. A summary of their work in a review paper by these authors [4] showed a falloff in power within one min. using an Al-electrode on the face of the module with bias of −1000 V to the cell at 85 °C. Also, for PERT cell mini modules, Luo and coworkers found PID-p to saturate in the 4–5 h timeframe when testing with bias of −1000 V applied to the cells at 40 °C under illumination, included to better simulate real-world conditions. Testing of the passivated rear of PERC cells in the dark, these authors found 40–45% power loss in 24 h, but simultaneously adding 10 W/m^2 or greater illumination on the cell back mitigated the PID-p. Testing of bifacial PERC modules in CAST “Spring” cycle which is a little under 2 days duration, including factors of voltage, temperature, moisture and full spectrum illumination, manifested in about 54% degradation when measured from the module rear, although other degradation mechanisms were occurring in parallel that contributed to the degradation measured [11]. Testing of the front face of PERT modules with −1000 V applied to cells at 60 °C with various resistivity and encapsulant levels showed PID-p in susceptible test samples reaching a maximum in up to 10 h, usually much less time [14]. Insofar as the rate of PID-p in field experiments, only the work of Ohdaira and coworkers testing PERT modules exists to our knowledge. They showed PID-p occurring and saturating within several 100 h of test and degrading no further in about 3 y timeframe; PID-p recovery could also be seen [6]. With TOPCon cells, stress testing with −1000 V bias at various temperatures in the dark showed saturation of PID-p in less than 150 h for temperatures 50 °C and above, and time to 5% degradation in less than about 35 h for accelerated testing in the range of 40–70 °C [16]. The results of these various accelerated and outdoor tests show the timeframe for rate of PID-p, appearing more like an infant failure mode. They also show PID-p saturates, beyond which the module degrades essentially no further by PID-p if the conditions don’t change significantly. In some cases, however, PID-p recovery can be observed depending on the module type and environmental conditions.

Above, we summarized various reports of rates of PID-p occurring in PERC and other technology modules, but it is critical to understand the actual field behavior of PERC modules with respect to PID-p, which has not yet been clarified. Because laboratory studies show small amounts (10 W/m^2 full spectrum light) incident on the bifacial PERC module rear can mitigate PID-p, there may be the assumption that such PID-p will not happen in elevated ground rack-mounted modules. We thus examine in this work if indeed PID-p occurs in fielded commercial bifacial PERC modules. Environmental factors known to affect PID-p rate such as temperature, humidity and irradiation are examined. Considering these parameters, especially those showing variability in the context of the outdoor testing performed herein, semi-empirical modeling is applied to validate the influence of the stress factors on PID-p rate.

2 Materials and methods

In this work, we first evaluated commercial 420 W (nominal) bifacial glass/glass PERC modules with ethylene vinyl acetate (EVA) encapsulant for PID-p sensitivity with both positive and negative 1500 V applied to the cell circuit at 25 °C for 168 h in an environmental chamber according to method (b), the Al foil method in IEC TS 62804-1, “Test methods for the detection of potential-induced degradation − Crystalline silicon” [8,17]. After checking the extent of the susceptibility to PID-p in both polarities and confirming the absence of PID-shunting, replicas of this module type were placed in the field in the Köppen-Geiger humid subtropical climate of Cocoa Florida in various mounting configurations. We constructed a near ground rack with the modules mounted about 30 cm above dirt that was supplied with water using an irrigation system that led to grass growth. Another was an elevated rack with modules mounted at about 2 m height, which had no irrigation system and a stable level of grass underneath it. In all cases, modules were mounted at an approximately 3° tilt from horizontal to avoid pooling of water on the modules. System voltage bias was applied logarithmically with irradiance to a maximum of 1500 V magnitude, similar to an apparatus previously described [18,19].

All modules were programmatically disconnected from the system voltage and subjected to IV sweeps approximately three times per day when the irradiance was stable; specifically, when the standard deviation of the irradiance of the previous minute was less than 2 W/m^2. These were performed in under 1 minute duration to minimize disconnection time from high voltage. Most modules had the temperature monitored with a thermocouple applied to the rear, and unbiased modules placed on all the above-mentioned racks for comparison (as outdoor controls) also had incident albedo measured on the rear with a downward facing Licor (LI-200R type) pyranometer. A single pyranometer for measuring plane of array (POA) irradiance was also mounted. Before application of system voltage bias to the modules connected to a load resistor circuit, the modules were placed on the racks self-biased for a period of three months. This preconditioning period is to resolve any quickly occurring degradation modes such as light-induced degradation and to achieve a natural level of

Table 1. Flash testing results under standard test condition (STC) of the front side of bifacial PERC modules for screening test of PID based on IEC 62804-1 (foil method). Only results on module faces that were stressed exhibiting degradation are shown. I_{sc} is the short circuit current, V_{oc}, open circuit voltage; *FF*, fill factor; and P_{max}, the maximum power point.

Test step	I_{sc} (A)	V_{oc} (V)	*FF* (%)	P_{max} (W)	% P_{max} change from initial	I_{sc} (A)	V_{oc} (V)	*FF* (%)	P_{max} (W)	% P_{max} change from initial
Stress level (25 °C 168 h, Al foil)		–1500 V (rear side stress)					+1500 V (front side stress)			
Initial	10.74	48.87	79.9	419.3	0	10.69	48.59	79.9	415.0	0
PID stress test	10.50	47.82	79.4	398.8	–4.9	10.57	47.96	79.3	402.1	–3.1
Intermediate recovery (storage)	10.11	46.78	78.8	372.6	–11.1					
Final recovery 19 kWh/m^2 illum.	10.71	48.83	79.8	417.1	–0.5	10.69	48.59	79.9	415.0	0

soiling before the start of the test that can affect surface conductivity of the glass [20]. Each rack type had three modules connected to the externally applied system voltage bias and one self-biased control. Because modules degrading by PID have changing temperature coefficients for their performance parameters [21], we do not calculate the degradation in power for each module by compensating for temperature and insolation. Instead, during periods of stable solar irradiance, IV sweeps of the externally biased PV modules are performed alongside the control while temporarily disconnecting them from the system voltage source with a relay network. After adjusting for initial differences in module power and actual irradiance measured by the pyrometer during the time of measurement of the module under bias and the control (within three minutes of one another), the power of the biased module is examined relative to that of the control. In this manner, issues other than PID induced by system voltage, including soling, light induced degradation, and UV-induced degradation, that would affect both voltage-stressed modules and the controls equivalently are largely eliminated from the power degradation calculation by this normalization process. Modules were also periodically removed from racks for electroluminescence imaging and for confirmation of module power by flash testing in the laboratory, as well as for evaluating the rate of recovery from PID-p at later stages that will be covered in separate publications. The back face of modules was covered with cardboard during dismounting for measurements to avoid any extraneous incident light. These measurements however confirmed for the purpose of this work that negligeable recovery could occur during the short disconnections of the module from system voltage bias when on-sun IV sweeps were taken.

To model the extent of PID-polarization according to the charge per unit area Q [coulombs/cm^2] in the dielectric causing it, a model that includes the rate of charge motion to the dielectric resulting from the voltage bias V (volts) and dissipation by photoconductivity proportional to the UV irradiation E [W/cm^2] was implemented (Eqs. (1)–(3)) [14]. V/ρ is effectively the current density through the packaging of thickness l [cm] transferred to the dielectric, where ρ [Ω-cm] is effective package resistivity. Charge transfer depends on material properties and environmental factors, especially module temperature and module surface wetness, which closes the circuit to ground permitting the current transfer. The dissipation by UV irradiation is a function of the existing charge available to be dissipated and a coefficient k [1/(W · s)].

$$\frac{dQ}{dt} = \frac{V}{\rho l} - kEQ. \tag{1}$$

Equation (1) is a linear first-order differential equation with solution for $Q(t)$,

$$Q(t) = \frac{V}{\rho lkE}\left(1 - e^{-kEt}\right). \tag{2}$$

A sigmoidal equation relating Q and the observed normalized power of a module taking the form

$$P_{max,norm}(Q) = (1 - P_\infty)\frac{A+1}{A+e^{BQ}} + P_\infty \tag{3}$$

is implemented with empirically determined terms A, which describes the latency for degradation after voltage bias is applied including built in charge to be overcome, B a factor describing the rate of degradation, and P_∞, the maximum extent of the degradation, which is believed associated with environmental and physical factors such as the extent of pre-existing states that can be charged (such as silicon nitride k-centers) [4] and the maximum rear surface recombination velocity experienced after the polarization [19,22].

3 Results

3.1 Screening test results

Results of accelerated stress testing to determine the sensitivity of the bifacial PERC module type used in this study with system voltage rating of 1500 V for evaluation of PID in the field based on IEC technical specification 62804-1

Table 2. Fielded modules under system voltage bias for the period 6.6.2023 to 18.12.2023 (d.m.y). Average values are given with corresponding calculated standard deviations in square brackets. Daytime values included are periods when system voltage is applied to the modules.

Rack type:	**Near ground**	**Elevated ground**	
Bias (V) (daytime):	−1500 V	−1500 V	+1500 V
Modules biased (controls):	3 (1)	3 (1)	3 (1)
Daytime module temperature (°C)	35.8 [11.4]	36.6 [11.5]	
Daytime module RH (%)	46.0 [25.9]	46.2 [26.4]	
Charge transferred (C/day)	0.012	0.007	
Albedo insolation kWh/m^2/day	0.240	0.376	

are shown in Table 1. These results are part of a broader previously published study (module "MB" in that study) [8], but the results relevant to this work are isolated here for conciseness. After negative voltage bias was applied to the cell circuit, placing the module in storage led to further degradation indicating the cells' rear were in inversion after the PID stress stage due to the positive charge buildup in the rear dielectric, as discussed in several previous reports [23,24]. These papers also show outsized degradation when flash tested from the rear because the minority carrier recombination is occurring at the back associated with PID-p occurring there. On the other hand, with the cell circuit in positive bias, the PID-p that occurs with development of net negative charge in the front dielectric attracting minority carrier holes in the front n-type emitter is less significant than the degradation on the back with negative bias. This is explained by the PERC back's lack of a diffused surface field leading to more sensitivity to positive charge buildup within the rear dielectric such that more minority carrier electrons in the *p*-type base recombine on the rear surface. In [8], the module type used in this work was also tested with the cell circuit in −1500 V, applying the potential over the front face at 25 °C for 168 h with Al foil electrodes. This resulted in −0.1% and −0.5% change in fill factor by flash testing the module front using 1000 and 200 W/m^2 respectively. This indicates negligeable PID-shunting sensitivity in the module type used in this work. Based on the PID-p sensitivities observed in the screening testing, replicas of this module type were chosen for field testing in configurations with system voltage in both polarities to understand their PID behavior in the field.

3.2 Field test results

Table 2 illustrates the differing mounting configurations of the fielded modules, the peak voltage bias applied during the day, the number of modules, the average daytime temperature and the average daytime relative humidity along with the standard deviation of these values, average daily cumulative coulombs transferred, and average daily albedo arriving on the module rear. These values collected are over a period of about six months to show the long-term behavior. The extent of grass under the near ground-mounted modules increased over the duration of the experiment, which would be anticipated to affect other factors, especially through reduction of albedo incident on the modules' back side.

Maximum power of modules (P_{max}) over time normalized to the unbiased controls for the three configurations listed in Table 2 are shown in Figure 1. The data marker types and colors respectively resolve the module and the time of day of the IV sweep for data collection. Data for all modules of a given rack elevation and electrical bias configuration are shown in aggregate here to see the overall trend; however, data for the individual degrading modules are given in Section 3.4. The data is resolved by time of day to see if there are any trends in PID-p or recovery over the course of a day. We do not perceive any systematic time of day dependency in the degrading modules. Degradation is seen within the first several weeks on the near ground and elevated ground rack modules after the start of application of −1500 V. There appears to be slightly slower degradation with modules in the elevated ground rack with negative bias, which is discussed in more detail below. No such immediate degradation is seen for the elevated ground rack modules in positive bias. Possible transient morning degradation with modules under +1500 V bias in elevated ground rack configuration may be seen but this behavior was not consistent among the modules in that configuration, so this observation requires further confirmation.

The degradation of modules in negative system voltage bias are seen to exhibit sustained PID-p whether mounted on the near ground or the elevated ground rack. These results are evidence of the occurrence of PID-p on the rear of bifacial PERC in field conditions, which has not been previously reported.

Figure 2a shows the development of I-V curves taken with a flash tester at standard test conditions (STC) two weeks before system voltage bias was turned on and 8 weeks

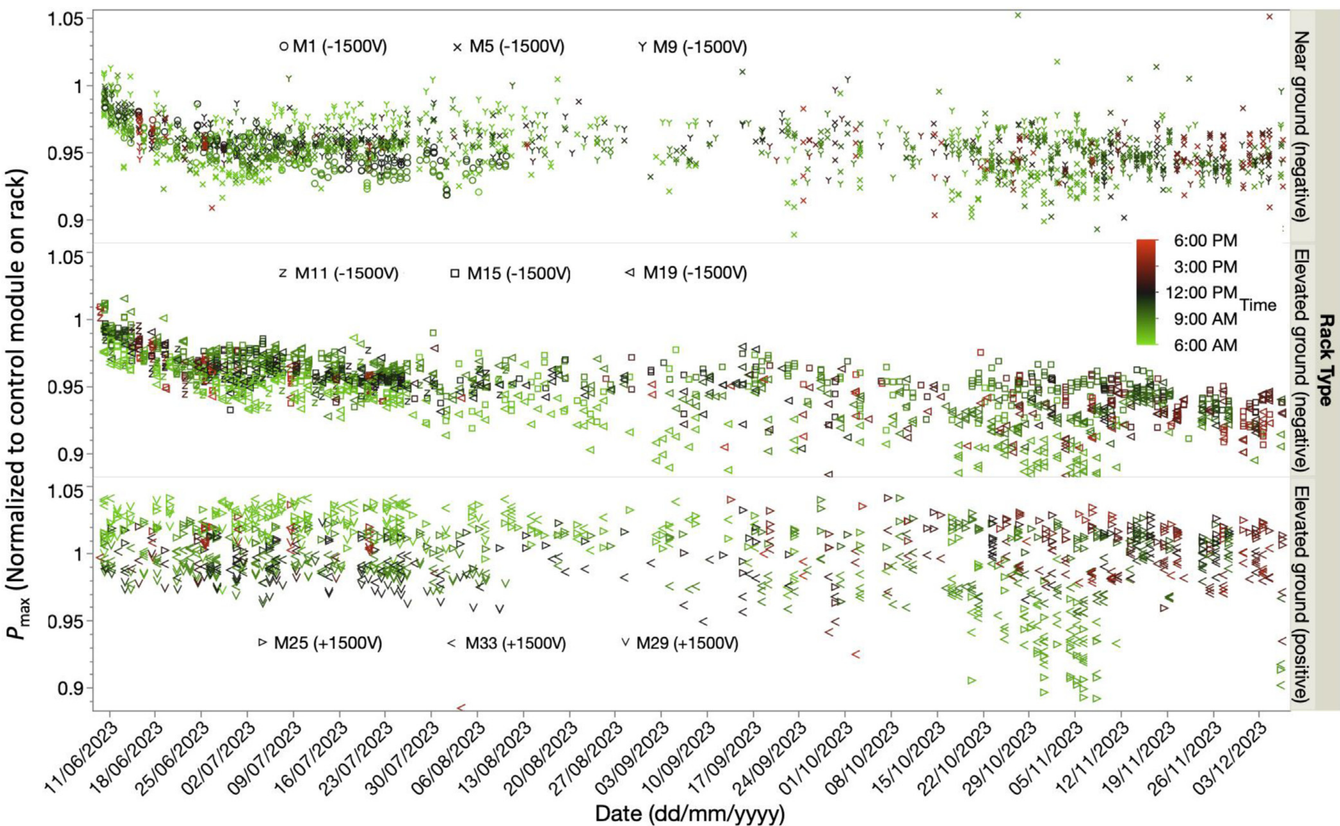

Fig. 1. Power of modules undergoing testing with 1500 V peak system voltage with polarities indicated on the plot, normalized to their control on three different rack types (mounting configurations) as a function of time. Symbol shapes indicate the sample number, color indicates the data collection time.

after system voltage bias was turned on. At 8 weeks of application of system voltage, corresponding to the first removal of modules from the rack starting on 1 August 2023, it can be seen from Figure 1 that the preponderance of degradation has already occurred. The near ground rack-mounted module in Figure 2a measured from the front shows no significant degradation in fill factor, which would be characteristic of PID-shunting mode [25,26]; therefore, PID-shunting by Na^+ migrating into the front junction [27,28] is not occurring. When this module subjected to system voltage bias in Figure 2a is flash tested from the rear, a significant decrease in short circuit current (I_{sc}) is observed over the course of the stress testing, consistent with PID-p occurring on the rear due to the increased effective surface recombination velocity occurring on the back of the bifacial PERC cell as previously characterized in accelerated stress testing, including with electroluminescence and external quantum efficiency measurements [2,11]. The I-V curves for the control module without voltage bias applied is shown in Figure 2b. This unbiassed control module also placed outdoors on the near ground rack showed about 0.6 mV loss in open circuit voltage (V_{oc}) measured from the front, which is expected from other simultaneously occurring mechanisms like, but not limited to, UV-induced degradation [29,30]. Further, leakage currents measured in the system that could lead to PID-p was found to correlate to atmospheric electric charges [31]. The rear of both the biased and control module showed instability in fill factor, which would be expected from cell mismatch stemming from factors including partial shading by the module frame and junction box.

3.3 Main effects

To model the degradation behavior, a study of the known controlling factors of PID-p and their magnitudes in the various mounting configurations is undertaken. Table 2 shows mean and standard deviations of daytime temperatures measured during the months of June through December. The near ground rack shows the lowest temperature followed by the elevated ground rack; however, the differences were marginal, with about 1 °C average incremental temperature difference.

Humidity was not directly monitored on the modules; however, surface relative humidity was calculated using the dew point and the module temperature [32]; the averages and standard deviations calculated are shown in Table 2. There is insignificant difference calculated between the relative humidity on the surfaces of modules mounted on the various racks; however, this calculation may not precisely capture the microclimates under the modules because meteorological station dew point is used, leaving only module temperature to influence the differences in module surface relative humidity that are calculated in Table 2.

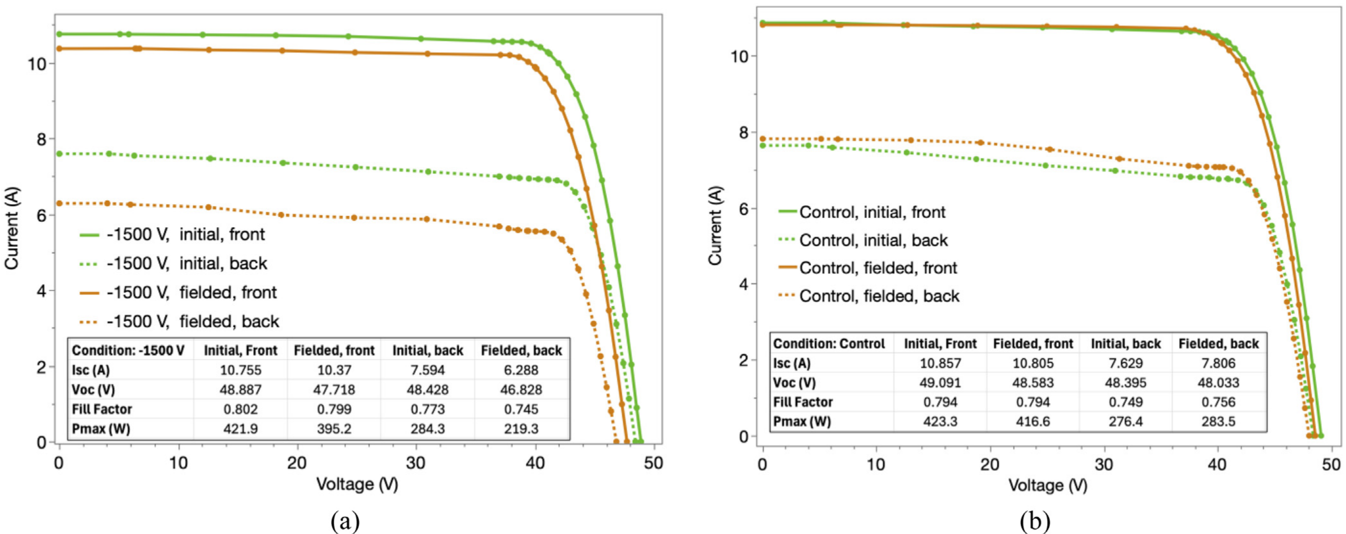

Fig. 2. Standard test condition flash testing measured from the front and back of modules mounted on the near ground rack with −1500 V system voltage, (a), and an unbiased control mounted alongside, (b). Initial measurements were taken two weeks before application of system voltage. Final flash test measurements shown were taken after approximately 8 weeks of application of system voltage in the test field. I_{sc} is the short circuit current, V_{oc}, open circuit voltage; and P_{max}, the maximum power point.

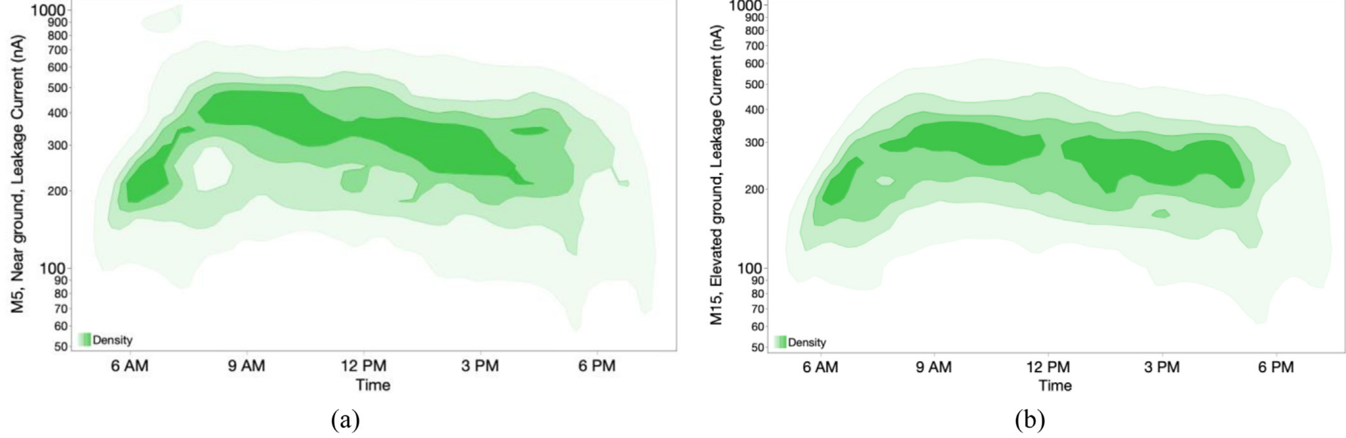

Fig. 3. Contour plot of leakage current from modules with (a) near ground and (b) elevated ground rack mounting displaying differing leakage current behavior over the time of day, with intensity proportional to the duration under the conditions. Data taken starting 6 June 2023 for 194 days duration.

While leakage current and resulting electrical charge transferred are not direct indicators of PID that may result, they are indicators of the effective PID stress resulting from voltage bias applied on the modules [13]. These tend to increase with humidity on the surface, which provides a conductive path across the module faces and temperature of the module because of ionic conduction through the module laminate that increases with temperature [33]. Average daily daytime leakage currents are shown in Table 2. Figure 3 shows a contour plot of leakage current as a function of time of day, comparing the modules that are mounted near ground to the elevated ground rack. Based on the figure, elevated leakage current appears during the period between around 6 PM to 10 AM, when the morning dew on the near ground rack-mounted module yields significant more leakage current than the elevated ground rack-mounted module over the approximately half a year period examined. For example, in the near ground rack-mounted module (Fig. 3a), leakage current approaches 1000 nA in the morning, which is not observed with the elevated ground rack-mounted module (Fig. 3b). Significant fraction of the electrical charge transferred from modules over the course of a day have been previously quantified during periods of morning dew on other module types in the humid subtropical environment [34,35].

While the results over the first six months of test summarized in Table 2 and Figures 1 and 3 show the long-term trends, Figure 1 shows most of the PID-p occurring in the negatively biased modules in the first 2.5 weeks. Therefore, we must look at the main effects to explain the PID-p rate more carefully for this early period.

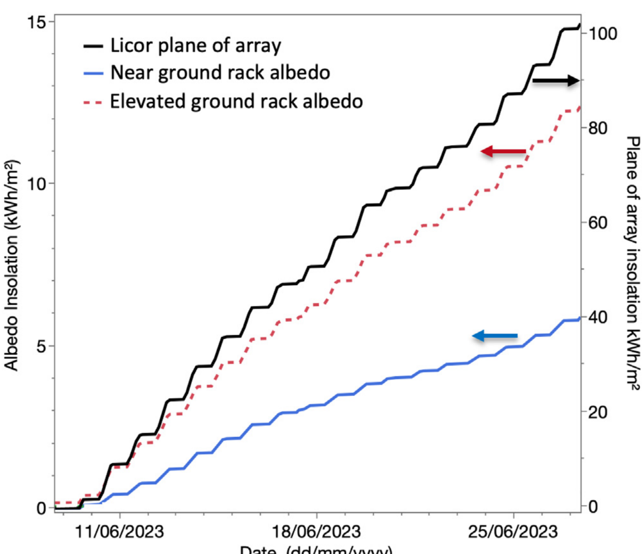

Fig. 4. Plane of array accumulated solar insolation and albedo incident on module back for modules on each of the rack types. Arrows point to the appropriate axis scale.

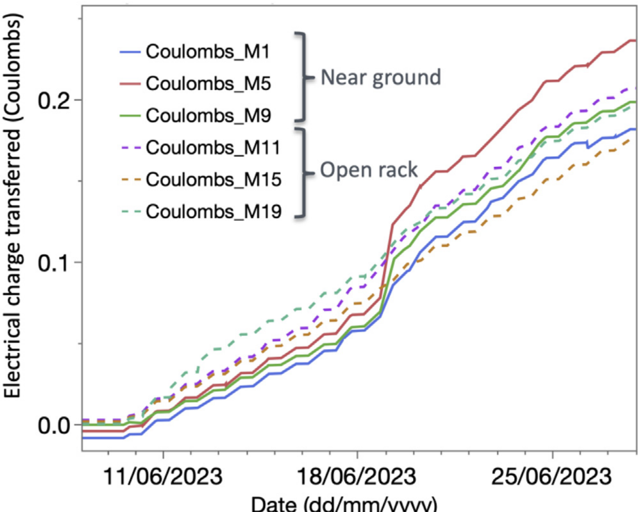

Fig. 5. Electrical charge transferred for the near ground and elevated ground rack modules, shown for period exhibiting fall in power due to potential-induced degradation-polarization.

Numerous papers indicate that solar irradiation, especially the portion in the UV band, dissipates PID-p-causing charge [5,7,14], therefore irradiation is examined here in more detail as a potential modulator of rate and extent of PID-p occurring in the various racks. Figure 4 shows the POA accumulated solar insolation and on module rears for each of the rack types. Focusing here on the first 2.5 weeks where PID-p was primarily occurring, we see about twice the accumulated albedo insolation on the elevated ground rack modules than the near ground modules. The different mounting configurations therefore exert an important influence on albedo, which in turn potentially affects PID-p rate through its known charge dissipating effects.

An additional major factor influencing PID-p is leakage current. Leakage current is highly sensitive to environmentally driven factors of module temperature and module relative humidity, which together leads to ionic conductivity through the module packaging [36]. This be seen with the exponential equation for accumulated charge over time (t) which has been previously found proportional to $e^{\frac{-E_a}{kT}} \cdot e^{RH\% \cdot B} \cdot t$ where E_a is the thermal activation energy, $RH\%$ is the equilibrium relative humidity, k the Boltzmann constant, and B a constant [13].

The accumulated electrical charge based on measured leakage current from the three near ground and three elevated ground rack modules over the first several weeks of deployment under bias is shown in Figure 5. Comparing the elevated ground and near ground rack-mounted modules during the period where most of the degradation happened, there is little difference in leakage current suggesting the net effect of differences of temperature and relative humidity of the modules on leakage current, a measure of the PID-causing stress on these modules, is not significant. In view of the results of Figures 4 and 5, the differences in rear side illumination appear much greater.

3.4 Modeling

In view of electrical charge transfer between modules mounted near ground and elevated ground rack being approximately the same according to Figure 5, the focus on modeling applying equations (1)–(3) is on the differences in albedo irradiation, the independent factor. Simplifying equation (3) for the purpose of curve fitting, grouping the constants with the environmental parameters so that they are a function of the differing rear side irradiance and substituting for the charge dependence on irradiance in equation (2), we have,

$$\frac{P_{max}}{P_0} = (1 - P_\infty)\frac{A+1}{A + \exp(B_1(1 - \exp(-Ct)))} + P_\infty \quad (4)$$

where $B_1 = \frac{BV}{\rho lkE}$, or essentially a factor proportional to the reciprocal of irradiance E considering the other parameters do not change significantly between the different modules and mounting configurations and where $C = kE$. Curve fitting for modules using equation (4) mounted near ground and elevated ground rack is shown in Figure 6.

The degradation curves given in Figure 1, which are broken out for each module individually in Figure 6, are not vastly different. Modules on the elevated ground rack however appear to degrade slower, especially M15 and M19. We seek to understand if the slower degradation rate is explained through the higher albedo incident on the module rear considering UV irradiation leads to photoconductivity and dissipation of charge in the cell rear dielectric. To this end, applying equation (4) and optimizing the fit with a Newton non-linear regression algorithm, parameter fits were obtained individually for each module given in Figure 6. The modelling was performed in the time (seconds) domain but is shown as days in the abscissa of Figure 6 for simplicity in viewing.

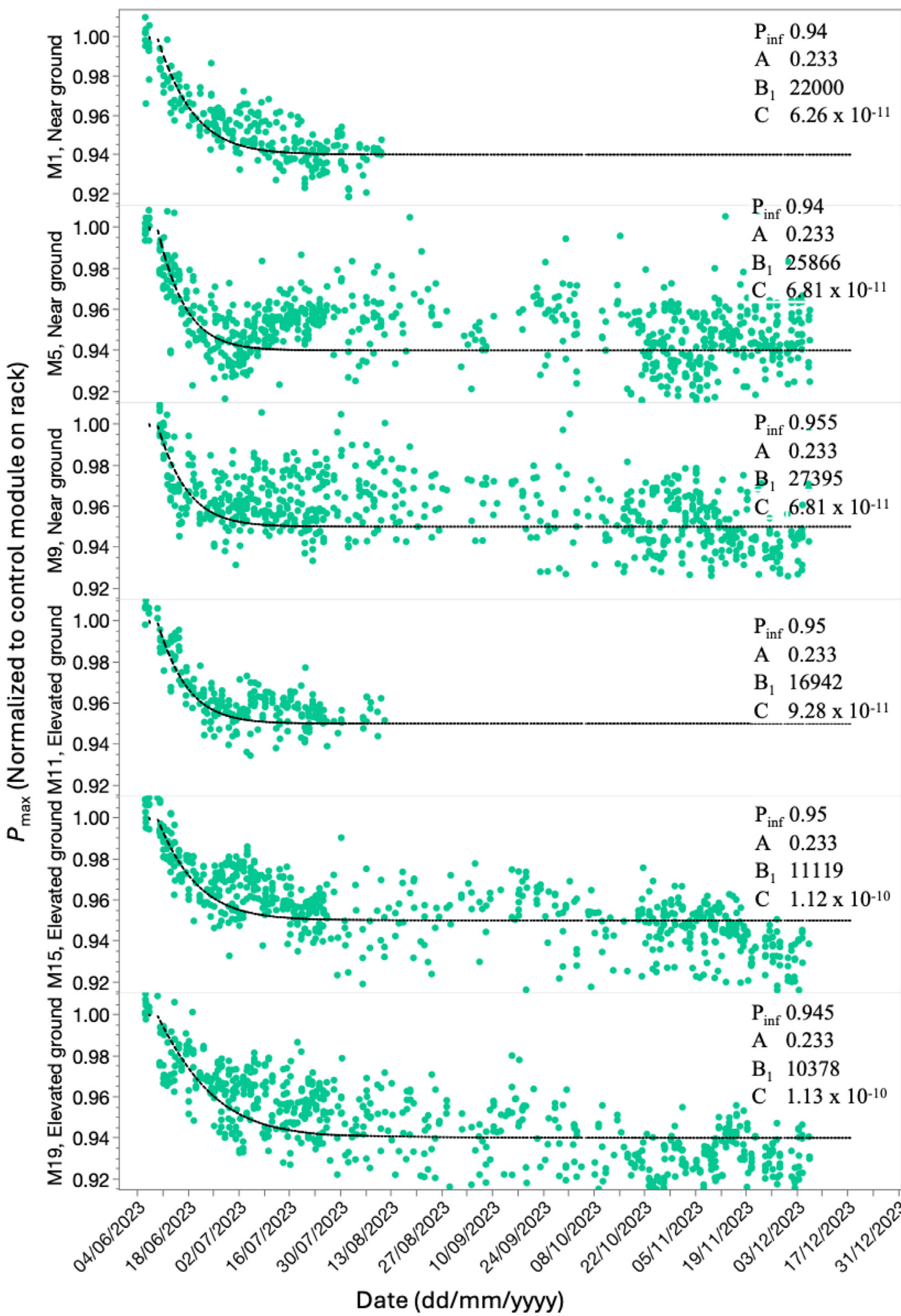

Fig. 6. Application of a sigmoidal model for $P_{\max}$ of various modules (normalized to unbiased control modules) as a function of time and rack type shown for the first 6 months after $-1500\,\text{V}$ peak system voltage applied. Testing of modules M1 and M11 terminated earlier due to system problems.

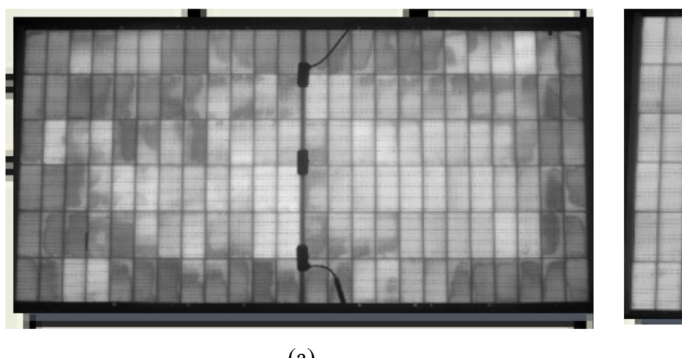

(a)

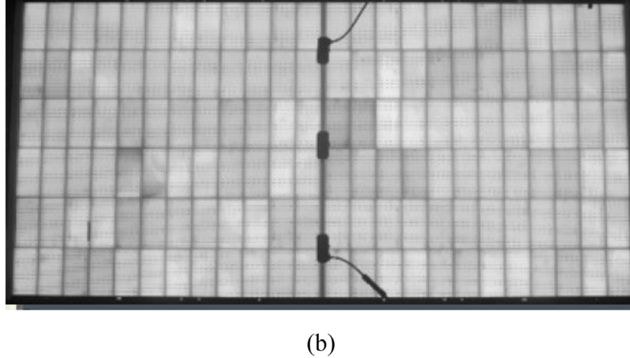

(b)

Fig. 7. Fielded module with −1500 V peak voltage applied, (a), compared to a fielded control after 10 weeks, (b), both mounted in elevated ground rack configuration at about 2 m elevation from the ground. Degradation attributable to potential-induced degradation-polarization type can be seen especially along the perimeter cells in (a).

The A parameter, which describes the extent of latency before degradation occurs did not differ much based on the regression and was consistently around 0.233. Consistent with that, negligeable latency can be distinguished—the degradation appears immediately after system voltage is applied. The ultimate power remaining P_∞ was set in the model based on the observed susceptibility of each individual module, but it can be seen in Figures 1 and 6 that the various P_∞ converge in the narrow range from 0.94 to 0.955 after the period of rapid degradation. B_1 and C parameter optimization was performed for the period of maximum degradation consistent with Figures 4 and 5, the first 2.5 weeks of tests. The B_1 parameter which goes with the reciprocal of irradiation averages 25807 for the near ground rack mounted modules, which compares with that of the elevated ground rack, 12813. The ratio of the B_1 parameter for near ground over that of elevated ground rack mounted modules is hence 1.96. The C parameter that is proportional to albedo incident on the module rear for elevated ground rack-mounted modules was found to be 1.06×10^{-10} and that of the near ground rack-mounted modules was 6.63×10^{-11} for a ratio of 1.60. These ratios are in agreement in the trend and direction, though not in absolute proportion with the rear side irradiation from albedo measured between the groups considering that the elevated ground rack-mounted modules 2 m in the air were measured to have approximately 2.1 more cumulative incident albedo than the near ground rack-mounted modules based on the data in Figure 5. Convoluting factors include that the irradiation sensors used record the broadband solar irradiance, whereas PID-p recovery is most dependent on the UV-band [7]. The proportion of UV to broadband irradiance changes with factors such as the grass growth [37].

3.5 Extent of PID-polarization

We seek to understand where in the PID-p process that the fielded modules seen in Figure 1 have saturated relative to the understanding previously introduced in the PID screening tests using aluminum foil given in Table 1. This informs whether the extent of PID-p could potentially be lesser or greater depending on the stress levels in differing field environments. For the modules under positive bias, in elevated ground rack, no apparent long-term degradation is seen, whereas in the screening test, PID-p could be seen because of degradation on the module front face. The positive voltage bias applied to the cell circuit can lead to a net negative charge buildup in the dielectric existing on top of the front n-type emitter, but perhaps because the PERC emitter on the module front is the primary sun facing side, there is sufficient dissipation of migrating charge by the insolation. Module fronts are not fundamentally immune to PID-p in the field however; published examples exist [1,6]. Occurrence is governed by a combination of factors such as the susceptibility of the cell, the module packaging electrical resistance to migrating charge, and climatic conditions on the affected module surfaces [14,15].

Under such accelerated stress testing with the cell circuit in negative potential given in Table 1, inversion of the energy bands in silicon on the back side of the cell may be observed and a reversion to increased conversion efficiency can result as stress continues to be applied [23,24]. The mean degradation over six-month period measured from the front side on sun with intermittent I–V tracing is in the range of 4.5–6% for all modules in negative voltage bias shown in Figures 1 and 6. Relating these results to the IEC 62804-1 screening tests in Table 1 for this module type, this is closer to the value for the inversion state of this module type, −4.9%, more so than an intermediate stage, −11.1%, where the Si base at the rear dielectric interface is near depletion.

For further insight, Figure 7 shows the electroluminescence after 8 weeks of field testing with negative voltage bias, here for the elevated ground rack-mounted module with −1500 V bias applied in comparison to an unbiased control. Understanding of the effects observed on the back of bifacial PERC undergoing PID-p with respect to the inversion process and the corresponding electroluminescence signature has been previously published [8,38]. Cells at the corner of the biased module in Figure 7a appear generally darker, where PID stresses are a maximum because of proximity to the grounded frame [39], suggesting those corner cells are not dominated by inversion. Further, the outer portion of the cells along the perimeter generally appear darker. If extensive inversion was to occur at the perimeter (the most highly stressed cells), they would appear brighter associated with a reversion to greater

efficiency. More work is necessary to relate the state of each of the cells in the module to the overall module power. There appears to be a range of PID-p states of the cells in modules subjected to negative system voltage bias in the field tests. Notably, M5 appears to undergo important trend in improvement of power at about 25 days of system voltage bias applied before exhibiting degradation again, which may be associated either with PID-p recovery or inversion. The degradation seen in the field was, to the extent measured, not varying much with mounting configuration or between module replicas within rack according to Figure 1.

System voltage rating refers to the maximum voltage between any two conductors in the system. By convention tranformerless ungrounded systems using 1500 V system voltage rated modules have modules with nominal system voltage between −750 V and +750 V at open-circuit voltage under low temperature conditions. The actual voltage is reduced yet further considering usual operating temperatures at maximum power. Still, there is a trend to greater system voltages so the effects observed here must be seriously considered. Further, there is variability in PID susceptibility inherent between module types and from different manufacturers. On the other hand, the extent of the degradation occurring on the back side of the bifacial PERC glass/glass modules measured with illumination from the front because of this PID-p mode measured herein are less in magnitude than with PID-p occurring in the field on the front as with older interdigitated back contact cells, up to −35% reported [1] and p^+n fronts of PERT degrading around −15% [6].

4 Conclusions

Screening of commercial bifacial glass/glass PERC modules showed both PID-p on the rear with cells in −1500 V bias and to a lesser extent on the front with the cells in +1500 V bias. The occurrence of PID-polarization of bifacial PERC modules with their rated system voltage −1500 V applied in the field was established. In field testing in the summer in a humid subtropical climate, such modules in negative bias degraded rapidly in a period of about 2.5 weeks, whereas module degradation could not be confirmed in the time period of about six months for those fielded in positive bias.

Comparing modules with −1500 V system voltage applied that were mounted in near ground and in elevated ground rack configurations, the rate of degradation was similar, but modules mounted near ground degraded with slightly faster apparent rate. During the initial, approximately 2.5-week period when most of the degradation occurred, the leakage current, which is a function of module temperature and relative humidity they experience, was approximately the same. However, albedo irradiation on the rear of the elevated ground rack modules with about 2 m elevation was about twice that of modules mounted near the ground with about 30 cm elevation. Modules mounted near the ground and in elevated ground rack degraded to about the same extent, 4.5% to 6%, and then largely stabilized at this level. Applying a sigmoidal model describing module power as a function charge incoming from the negative voltage applied and countered by dissipation from incident irradiation, the effect of irradiation was quantified. The coefficients indicted the irradiance on the rear were 1.96 and 1.6 times greater for the elevated ground rack module compared to the near ground rack module, reasonably matching the measured accumulated albedo ratio incident on the module rear of about 2.1.

Acknowledgments

The authors thank Mr. Joe Walters for important assistance in acquiring project funding and initial help in project management before departing the project.

Funding

This material is based upon work supported by the U.S. Department of Energy's Office of Energy Efficiency and Renewable Energy (EERE) under the Solar Energy Technologies Office Award Number DEEE0009345. This work is also part of the SETO Project 38263. This report was prepared as an account of work sponsored by an agency of the United States Government. Neither the United States Government nor any agency thereof, nor any of their employees, makes any warranty, express or implied, or assumes any legal liability or responsibility for the accuracy, completeness, or usefulness of any information, apparatus, product, or process disclosed, or represents that its use would not infringe privately owned rights. Reference herein to any specific commercial product, process, or service by trade name, trademark, manufacturer, or otherwise does not necessarily constitute or imply its endorsement, recommendation, or favoring by the United States Government or any agency thereof. The views and opinions of authors expressed herein do not necessarily state or reflect those of the United States Government or any agency thereof. The U.S. Government retains and the publisher, by accepting the article for publication, acknowledges that the U.S. Government retains a nonexclusive, paid-up, irrevocable, worldwide license to publish or reproduce the published form of this work, or allow others to do so, for U.S. Government purposes.

Conflicts of interest

The authors declare no conflicts of interest.

Data availability statement

Reasonable requests for data by email to the authors will be accommodated.

Author contribution statement

Conceptualization, all authors; methodology, all authors; validation, C. Molto; formal analysis, P. Hacke, C. Molto, F.I. Mahmood; investigation, all authors; resources, all authors; data curation, all authors; writing – original draft preparation, P. Hacke; writing – review & editing, C. Molto and F. Li; visualization, all authors; supervision, P. Hacke, R. Smith,

G. Tamizhmani, and H. Seigneur; project administration, H. Seigneur; funding acquisition, P. Hacke, G. Tamizhmani, and H Seigneur.

References

1. R. Swanson, M. Cudzinovic, D. DeCeuster, V. Desai, J. Jürgens, N. Kaminar, W. Mulligan, L. Rodrigues-Barbarosa, D. Rose, D. Smith, The surface polarization effect in high-efficiency silicon solar cells, in *15th PVSEC* (Shanghai, China, 2005)
2. W. Luo, P. Hacke, K. Terwilliger, T.S. Liang, Y. Wang, S. Ramakrishna, A.G. Aberle, Y.S. Khoo, Elucidating potential-induced degradation in bifacial PERC silicon photovoltaic modules, Prog. Photovolt.: Res. Appl. **26**, 859 (2018)
3. W. Luo, P. Hacke, J.P. Singh, J. Chai, Y. Wang, S. Ramakrishna, A.G. Aberle, Y.S. Khoo, In-situ characterization of potential-induced degradation in crystalline silicon photovoltaic modules through dark I-V measurements, IEEE J. Photovolt. **7**, 104 (2017)
4. S. Yamaguchi, B.B. Van Aken, A. Masuda, K. Ohdaira, Potential-induced degradation in high-efficiency n-type crystalline-silicon photovoltaic modules: a literature review, Sol. RRL **5**, 2100708 (2021)
5. R.M. Swanson, D. De Ceuster, V. Desai, D.H. Rose, D.D. Smith, N. Kaminar, Preventing harmful polarization of solar cells, US Patent (2009)
6. K. Ohdaira, M. Akitomi, Y. Chiba, A. Masuda, Potential-induced degradation of *n*-type front-emitter crystalline silicon photovoltaic modules—comparison between indoor and outdoor test results, Sol. Energy Mater. Sol. Cells **249**, 112038 (2023)
7. W. Luo, P. Hacke, S.M. Hsian, Y. Wang, A.G. Aberle, S. Ramakrishna, Y.S. Khoo, Investigation of the impact of illumination on the polarization-type potential-induced degradation of crystalline silicon photovoltaic modules, IEEE J. Photovolt. **8**, 1168 (2018)
8. F.I. Mahmood, F. Li, P. Hacke, C. Molto, D. Colvin, H. Seigneur, G. Tamizhmani, Susceptibility to polarization type potential induced degradation in commercial bifacial p-PERC PV modules, Progr. Photovolt.: Res. Appl. **31**, 1078 (2023)
9. C. Molto, J. Oh, F.I. Mahmood, M. Li, P. Hacke, F. Li, R. Smith, D. Colvin, M. Matam, C. DiRubio, Review of potential-induced degradation in bifacial photovoltaic modules, Energy Technol. **11**, 2200943 (2023)
10. D.B. Sulas-Kern, M. Owen-Bellini, P. Ndione, L. Spinella, A. Sinha, S. Uličná, S. Johnston, L.T. Schelhas, Electrochemical degradation modes in bifacial silicon photovoltaic modules, Prog. Photovolt.: Res. Appl. **30**, 948 (2022)
11. P. Hacke, A. Kumar, K. Terwilliger, P. Ndione, S. Spataru, A. Pavgi, K.R. Choudhury, G. Tamizhmani, Evaluation of bifacial module technologies with combined-accelerated stress testing, Progr. Photovolt.: Res. Appl. **31**, 1270 (2023)
12. J. Hattendorf, R. Loew, W. Gnehr, L. Wulff, M. Koekten, D. Koshnicharov, A. Blauaermel, J. Esquivel, Potential induced degradation in mono-crystalline silicon based modules: an acceleration model, in *Proceedings of the 27th European PV Solar Energy Conference* (Frankfurt, Germany, 2012), pp. 3405–3410
13. P. Hacke, S. Spataru, K. Terwilliger, G. Perrin, S. Glick, S. Kurtz, J. Wohlgemuth, Accelerated testing and modeling of potential-induced degradation as a function of temperature and relative humidity, IEEE J. Photovolt. **5**, 1549 (2015)
14. B.M. Habersberger, P. Hacke, Impact of illumination and encapsulant resistivity on polarization-type potential-induced degradation on n-PERT cells, Progr. Photovolt.: Res. Appl. **30**, 455 (2022)
15. B.M. Habersberger, P. Hacke, Measuring and modeling the rate of power loss in N-PERT cells associated with PID-P as a function of encapsulant resistivity and irradiance, in *WCPEC-8* (Milan, 2022), pp. 939–942
16. P. Hacke, S. Spataru, B. Habersberger, Y. Chen, Field-representative evaluation of PID-polarization in TOPCon PV modules by accelerated stress testing, Progr. Photovolt.: Res. Appl. **32**, 346 (2024)
17. IEC 62804–1 Photovoltaic (PV) modules – Test methods for the detection of potential-induced degradation – Part 1: Crystalline silicon, IEC, Genvea (2015)
18. P. Hacke, S. Johnston, W. Luo, S. Spataru, R. Smith, I. Repins, Prediction of potential-induced degradation rate of thin-film modules in the field based on Coulombs transferred, in *2018 IEEE 7th World Conference on Photovoltaic Energy Conversion (WCPEC)(A Joint Conference of 45th IEEE PVSC, 28th PVSEC & 34th EU PVSEC)* (IEEE, Waikoloa Village, 2018), pp. 3801–3806
19. P. Hacke, R. Smith, K. Terwilliger, G. Perrin, B. Sekulic, S. Kurtz, Development of an IEC test for crystalline silicon modules to qualify their resistance to system voltage stress, Prog. Photovolt.: Res. Appl. **22**, 775 (2014)
20. P. Hacke, P. Burton, A. Hendrickson, S. Spataru, S. Glick, K. Terwilliger, Effects of photovoltaic module soiling on glass surface resistance and potential-induced degradation, in *Photovoltaic Specialist Conference (PVSC) 2015 IEEE 42nd* (IEEE, 2015), pp. 1–4
21. R. Desharnais, Characterizing the impact of potential-induced degradation and recovery on the irradiance and temperature dependence of photovoltaic modules, in *29th European Photovoltaic Solar Energy Conference and Exhibition* (2014)
22. B.M. Habersberger, P. Hacke, L.S. Madenjian, Evaluation of the PID-s susceptibility of modules encapsulated in materials of varying resistivity, in *2018 IEEE 7th World Conference on Photovoltaic Energy Conversion (WCPEC)(A Joint Conference of 45th IEEE PVSC, 28th PVSEC & 34th EU PVSEC)* (IEEE, 2018), pp. 3807–3809
23. W. Luo, P. Hacke, K. Terwilliger, T.S. Liang, Y. Wang, S. Ramakrishna, A.G. Aberle, Y.S. Khoo, Elucidating potential-induced degradation in bifacial PERC silicon photovoltaic modules, Progr. Photovolt.: Res. Appl. **26**, 859 (2018)
24. K. Sporleder, V. Naumann, J. Bauer, D. Hevisov, M. Turek, S. Dittmann, C. Hagendorf, Fast changing field effect passivation states due to potential induced degradation at the rear side of bifacial silicon solar cells, AIP Conf. Proc. **2487**, 030011-1 (2022)
25. G. Mathiak, M. Schweiger, W. Herrmann, Potential-induced degradation—Comparison of different test methods and low irradiance performance measurements, in *27th European Photovoltaic Solar Energy Conference and Exhibition* (2012), pp. 3157–3162

26. P. Hacke, K. Terwilliger, S. Kurtz, In-situ measurement of crystalline silicon modules undergoing potential-induced degradation in damp heat stress testing for estimation of low-light power performance, National Renewable Energy Lab. (NREL), Golden, CO (United States) (2013)
27. S.P. Harvey, J. Moseley, A. Norman, A. Stokes, B. Gorman, P. Hacke, S. Johnston, M. Al-Jassim, Investigating PID shunting in polycrystalline silicon modules via multiscale, multitechnique characterization, Progr. Photovolt.: Res. Appl. **26**, 377 (2018). https://doi.org/10.1002/pip.2996
28. V. Naumann, D. Lausch, A. Hähnel, J. Bauer, O. Breitenstein, A. Graff, M. Werner, S. Swatek, S. Großer, J. Bagdahn, Explanation of potential-induced degradation of the shunting type by Na decoration of stacking faults in Si solar cells, Sol. Energy Mater. Sol. Cells **120**, 383 (2014)
29. A. Sinha, J. Qian, S.L. Moffitt, K. Hurst, K. Terwilliger, D.C. Miller, L.T. Schelhas, P. Hacke, UV-induced degradation of high-efficiency silicon PV modules with different cell architectures, Progr. Photovolt. **31**, 36 (2022)
30. R. Witteck, B. Veith-Wolf, H. Schulte-Huxel, A. Morlier, M.R. Vogt, M. Köntges, R. Brendel, UV-induced degradation of PERC solar modules with UV-transparent encapsulation materials, Progr. Photovolt.: Res. Appl. **25**, 409 (2017)
31. C. Molto, R. Smith, D.J. Colvin, P. Hacke, C. DiRubio, M. Gardeski, F. Li, J. Oh, G. Tamizhmani, C. Raupp, Field study of nighttime leakage currents in bifacial pv modules: correlation with atmospheric electric field data, in *2024 IEEE 52nd Photovoltaic Specialist Conference (PVSC)* (IEEE, 2024), pp. 0368–0372
32. O.A. Alduchov, R.E. Eskridge, Improved Magnus form approximation of saturation vapor pressure, J. Appl. Meteorol. **35**, 601 (1996)
33. J. Del Cueto, T. McMahon, Analysis of leakage currents in photovoltaic modules under high-voltage bias in the field, Progr. Photovolt.: Res. Appl. **10**, 15 (2002)
34. P. Hacke, K. Terwilliger, R. Smith, S. Glick, J. Pankow, M. Kempe, S.K.I. Bennett, M. Kloos, System voltage potential-induced degradation mechanisms in PV modules and methods for test, in *Photovoltaic Specialists Conference (PVSC), 2011 37th IEEE* (IEEE, 2011), pp. 000814–000820
35. P. Hacke, R. Smith, S. Kurtz, D. Jordan, J. Wohlgemuth, Modeling current transfer from PV modules based on meteorological data, in *Photovoltaic Specialists Conference (PVSC), 2016 IEEE 43rd* (IEEE, 2016), pp. 1083–1089
36. J. Berghold, S. Koch, B. Frohmann, P. Hacke, P. Grunow, Properties of encapsulation materials and their relevance for recent field failures, in *Photovoltaic Specialist Conference (PVSC), 2014 IEEE 40th (*IEEE, Denver, CO, 2014), pp. 1987–1992
37. R. Chadyšiene, A. Girgždys, Ultraviolet radiation albedo of natural surfaces, J. Environ. Eng. Landscape Manag. **16**, 83 (2008)
38. K. Sporleder, V. Naumann, J. Bauer, D. Hevisov, M. Turek, C. Hagendorf, Time-resolved investigation of transient field effect passivation states during potential-induced degradation and recovery of bifacial silicon solar cells, Sol. RRL **5**, 2100140 (2021)
39. N. Shiradkar, E. Schneller, N.G. Dhere, Finite element analysis based model to study the electric field distribution and leakage current in PV modules under high voltage bias, in *Reliability of Photovoltaic Cells, Modules, Components, and Systems VI* (SPIE, 2013), pp. 101–109

Cite this article as: Peter Hacke, Cecile Molto, Dylan Colvin, Ryan Smith, Farrukh Ibne Mahmood, Fang Li, Jaewon Oh, Govindasamy Tamizhmani, Hubert Seigneur, Polarization-type potential-induced degradation in bifacial PERC modules in the field, EPJ Photovoltaics **16**, 16 (2025), https://doi.org/10.1051/epjpv/2025004